JACS
JOURNAL OF THE AMERICAN CHEMICAL SOCIETY
pubs.acs.org/JACS
Article

Solvent Isotope Effects on the Creation of Fluorescent Quantum Defects in Carbon Nanotubes by Aryl Diazonium Chemistry

Brandon J. Heppe, Nina Dzombic, Joseph M. Keil, Xue-Long Sun,* and Geyou Ao*

Cite This: J. Am. Chem. Soc. 2023, 145, 25621−25631
Read Online
ACCESS | Metrics & More | Article Recommendations | Supporting Information

ABSTRACT: The integration of aryl diazonium and carbon nanotube chemistries has offered rich and versatile tools for creating nanomaterials of unique optical and electronic properties in a controllable fashion. The diazonium reaction with single-wall carbon nanotubes (SWCNTs) is known to proceed through a radical or carbocation mechanism in aqueous solutions, with deuterated water (D_2O) being the frequently used solvent. Here, we show strong water solvent isotope effects on the aryl diazonium reaction with SWCNTs for creating fluorescent quantum defects using water (H_2O) and D_2O. We found a deduced reaction constant of ∼18.2 times larger value in D_2O than in H_2O, potentially due to their different chemical properties. We also observed the generation of new defect photoluminescence over a broad concentration range of diazonium reactants in H_2O, as opposed to a narrow window of reaction conditions in D_2O under UV excitation. Without UV light, the physical adsorption of diazonium on the surface of SWCNTs led to the fluorescence quenching of nanotubes. These findings provide important insights into the aryl diazonium chemistry with carbon nanotubes for creating promising material platforms for optical sensing, imaging, and quantum communication technologies.

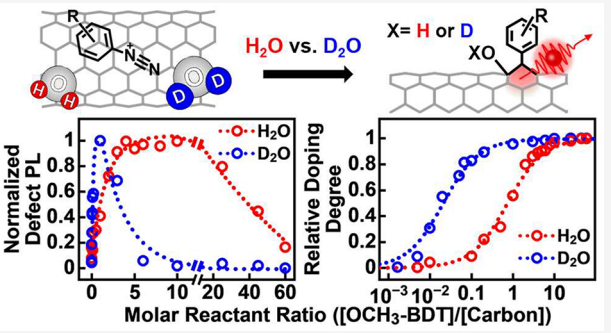

INTRODUCTION

The rich chemistry of carbon nanotubes has created diverse electronic structures and optical properties. Particularly, the aryl diazonium chemistry with single-wall carbon nanotubes (SWCNTs) has enabled versatile synthesis ranging from the selective reaction of metallic SWCNTs[1−4] to the creation of organic color centers (OCCs) in semiconducting SWCNTs.[5−10] The latter is known to covalently attach aryl functional groups and pairing groups, such as −H or −OH in an aqueous environment, or another aryl dopant, to the same carbon ring on the sp^2 carbon lattice, thereby creating fluorescent sp^3 quantum defects at a low functionalization density.[8,11−13] These sp^3 defects on the SWCNT surface perturb the electronic structure of the functionalized nanotubes by reducing the energy gaps, which further modifies the optical properties.[7,14] It is particularly promising that such fluorescent defects can trap diffusing excitons, thereby producing bright and red-shifted defect photoluminescence (PL) in a broad spectral window further into the near-infrared (NIR, >1100 to 1600 nm) region. The diverse structures and properties of OCC-tailored SWCNTs offer numerous merits for biosensing and imaging with increased sensitivity and resolution in the tissue transparent optical window[15,16] and for telecom communication due to their single-photon emission at room temperature.[17,18]

The defect-state optical features of OCC-tailored SWCNTs can be tuned by controlling the (*n*,*m*) SWCNT chiralities, functional groups (i.e., electron withdrawing capability), bonding configurations (i.e., ortho versus para positions) of pairing groups and their reconfigurations by laser irradiations, as well as the nucleophilic solvent structures.[8,9,19−22] A recent report by Wang and colleagues indicated that aryl diazonium reactions proceed through the formation of carbocations in chlorosulfonic acid rather than a radical mechanism that typically occurs in aqueous solutions. In particular, water plays an unexpected role in completing the diazonium reaction with carbon nanotubes involving chlorosulfonic acid, acting as a nucleophilic agent that contributes −OH as the pairing group to form a covalent bond that completes the OCC defect pair.[8] In aqueous environments, the aryl diazonium reaction with SWCNTs is generally believed to proceed through a carbon radical-mediated pathway, where a species from either water solvent or another reactant is captured as a pairing group.[3,6,23] Additionally, water can affect radical formation and diazonium or aryl radical decompositions. In fact, H_2O and D_2O are often used to obtain important information about the role of water in the reaction and reaction mechanism.[24] For example, H_2O and D_2O show different effects on the radical stability as an

Received: July 12, 2023
Revised: October 17, 2023
Accepted: October 30, 2023
Published: November 16, 2023

https://doi.org/10.1021/jacs.3c07341
J. Am. Chem. Soc. 2023, 145, 25621−25631

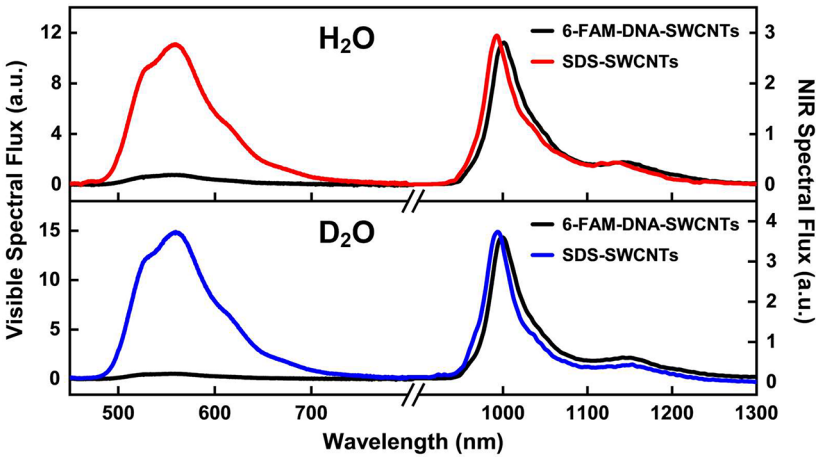

Figure 1. Displacement of 6-FAM-DNA coating from (6,5) SWCNTs by SDS. Visible and NIR fluorescence spectra of 6-FAM fluorophore and (6,5) SWCNTs before (i.e., 6-FAM-DNA-SWCNTs) and after (i.e., SDS-SWCNTs) surfactant exchange in H_2O (top) and D_2O (bottom), respectively. Fixed excitation wavelengths of 408 and 532 nm lasers were used for acquiring visible and NIR fluorescence spectra of 6-FAM dye and SWCNTs, respectively.

increased effective lifetime of radicals was observed for species of photoproduced cation radicals that were embedded in surfactant micelles when replacing H_2O with D_2O.[25] Therefore, water solvent isotope effects may impact the aryl diazonium reaction with surfactant-coated SWCNTs in creating OCC-SWCNTs. However, a direct comparison of the different reaction behaviors of aryl diazonium with SWCNTs in solvent waters of H_2O and D_2O has been missing. This hampers the potential of further diversifying the nanotube chemistry by integrating precise biological functionalities onto OCC-tailored SWCNTs using bioorthogonal chemistry, which generally requires benign aqueous conditions.[26,27] Achieving this will further enable the synthesis and biomedical applications of OCC-tailored SWCNTs with unique optical and biological functionalities under aqueous conditions.

Additionally, covalent functionalization of SWCNTs can be significantly accelerated by light (i.e., ultraviolet (UV) or visible light) that excites either the SWCNTs[28,29] or the aromatic reactants, including aryl diazonium.[30,31] A previous report by Wang and colleagues showed that functionalization of SWCNTs using diazonium salts could be accelerated by roughly 154-fold, through visible light excitation of the carbon nanotubes.[28] Aryl diazonium salts are known to absorb light at wavelengths between 290 and 360 nm.[32−34] After excitation, nitrogen is extruded from aryl diazonium, a process called photodissociation, in which aryl radicals can be formed.[35,36] In this work, we performed the aryl diazonium chemistry of pure-chirality (6,5) SWCNTs by irradiating mixtures of SWCNTs and diazonium reactants with UV light in isotopic waters of H_2O and D_2O in an attempt to obtain important information about the role of water. We found that the deduced reaction constant in D_2O is roughly 18.2 times larger than that in H_2O, indicating the potential solvent isotope effects on the reaction. We also observed a stable, bright defect PL in H_2O over the broad concentration range of diazonium tested, as compared to a narrow window of reaction conditions in D_2O. Additionally, we demonstrate a distinct two-step reaction involving the possible physical adsorption of cationic diazonium reactants onto the anionic surfactant-coated SWCNTs, followed by the covalent bonding of defect color centers on the SWCNT carbon lattice with UV excitation. This study adds an important piece to the drastically expanding chemistry toolbox for controlling quantum defects on graphitic carbons.

RESULTS AND DISCUSSION

To create OCC-tailored SWCNTs, we used anionic surfactant sodium dodecyl sulfate (SDS)-coated SWCNTs that were produced by surfactant exchange in 1 mass% SDS in solvent H_2O and D_2O, respectively, to displace the resolving DNA sequence (i.e., TTA TAT TAT ATT) on the pure-chirality (6,5) SWCNTs, according to our previously reported procedure.[37] We observed minor solvatochromic shifts (i.e., spectral blue shifts) of roughly 3 nm for the pristine E_{11} emission of DNA-(6,5) SWCNTs (near 994 nm), while the E_{11} photoluminescence (PL) remained similar after displacing DNA coating by SDS in both solvent waters, which is likely due to the similar surface coverage of nanotubes created by these two coating materials (Figure 1, Figure S1, and Table S1). SDS is known to stabilize SWCNTs in aqueous environment by forming sparse, disordered micellar structures on the nanotube surface.[1,4,38] Additionally, we performed the surfactant exchange using the resolving DNA sequence containing visible fluorophore 6-carboxyfluorescein (6-FAM) conjugated to the 3′ end to further validate the displacement of the DNA coating from the SWCNT surface by SDS (Figure 1 and Figure S2). The fluorescence of aromatic fluorophores is known to quench when they adsorb onto the SWCNT surface through hydrophobic interactions, while becoming highly fluorescent upon detachment from the SWCNTs.[39−41] As expected, we observed a significant increase of 6-FAM fluorescence at 560 nm peak after DNA/SDS exchange in both solvent waters, while the pristine E_{11} PL of (6,5) SWCNTs showed no obvious change, confirming the displacement of DNA by SDS from the nanotube surface (Figure 1).

SDS is also known to stabilize diazonium salts to a certain extent in an aqueous environment.[3] With the presence of 1 mass% SDS, we observed negligible changes in the absorption of 4-methoxybenzenediazonium tetrafluoroborate (i.e., OCH_3-BDT) in both H_2O and D_2O after being kept in the dark for 50 min, which corresponds to the time period used for the aryl diazonium reaction with SWCNTs (Figures S3). We primarily utilized OCH_3-BDT to react with SDS-coated SWCNTs containing 1 mass% SDS under UV light (i.e., 302 nm

https://doi.org/10.1021/jacs.3c07341
J. Am. Chem. Soc. 2023, 145, 25621−25631

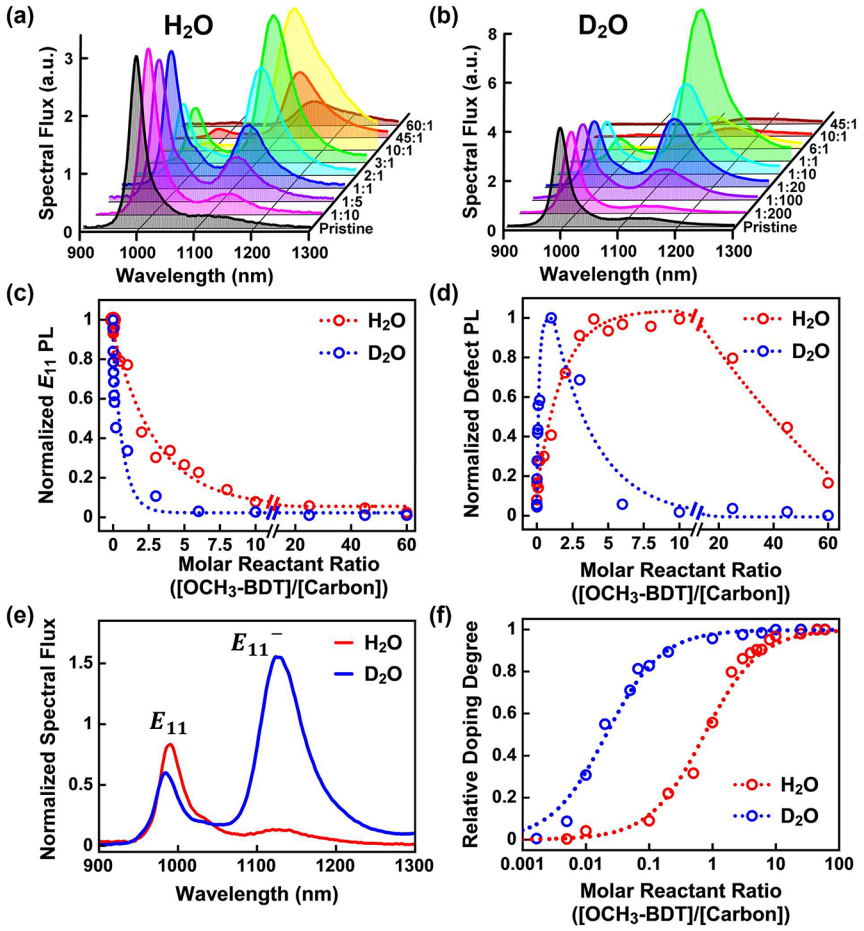

Figure 2. Solvent-dependent aryl diazonium reaction of (6,5) SWCNTs with 4-methoxybenzenediazonium tetrafluoroborate. Fluorescence spectra of $C_6H_4OCH_3$-OCC-tailored-(6,5) SWCNTs created in (a) H_2O and (b) D_2O, respectively, at various molar ratios of [OCH_3-BDT]:[SWCNT carbon] with 302 nm UV light irradiation for 50 min. The corresponding normalized intensities of (c) pristine E_{11} (near 988 nm) and (d) defect PL (near 1131 nm) peaks. The dotted lines in parts c and d represent the fitting curves with $R^2 \approx 95.4\%$ using single exponential fits (i.e., $y = Ae^{-kx} + B$, where A and B are correction factors). (e) Normalized fluorescence spectra of SWCNTs at [OCH_3-BDT]:[SWCNT carbon] = 1:10. (f) Relative doping degree of (6,5) SWCNTs with increasing molar reactant ratios. The dotted lines in panel f represent the fitting curves with $R^2 >$ 98.6% using the two-step adsorption−reaction model.

wavelength) irradiation at ambient conditions in solvent H_2O and D_2O, respectively. As mentioned above, optical excitation can accelerate covalent functionalization of SWCNTs with aryl diazonium as light (i.e., UV or visible light) can excite either the SWCNTs[28,29] or aryl diazonium.[30,31] The UV light used in this work is resonant with the diazonium UV absorption band (Figure S3 and S4).[32] We also synthesized 4-carboxylbenzene diazonium tetrafluoroborate salt (i.e., COOH-BDT) (Figure S5) to test the solvent effects on the aryl diazonium reaction with SWCNTs.

To analyze the relative doping degree of SWCNTs, we fitted the pristine E_{11} (near 988 nm) emission and the newly formed, red-shifted defect-state E_{11}^- (centered around 1131 nm) and E_{11}^-* (centered around 1210 nm) emission peaks of OCC-tailored SWCNTs using Voigt profiles (Figure S6). Additionally, we performed control experiments of UV irradiation of SDS-SWCNTs (without diazonium reactants) containing two different surfactant concentrations of 0.03 mass% (i.e., 1.05 mM), which is below the critical micelle concentration (CMC) of ~7 mM,[42] and 1 mass% (i.e., 34.6 mM) in H_2O and D_2O, respectively (Figures S7−S10). When irradiating SDS-SWCNTs containing 0.03 mass% SDS with higher-energy UV photon (i.e., 254 nm wavelength), we observed the oxygen doping of nanotubes in both solvents due to the exposure of SWCNT surface to reactive oxygen species in the solvent environment as reported previously by us (Figure S9a,b).[37] However, we did not observe obvious oxygen doping of SWCNT samples when using 1 mass% SDS (i.e., corresponding to nanotubes with higher surface coverage) and a longer wavelength of 302 nm UV light (Figure S9c,d and Figure S10). The UV absorption of molecular oxygen at various states generally occurs below 300 nm.[43] We also performed a control experiment by exciting the E_{22} optical transition peak of SWCNTs using a 532 nm laser to avoid potential photoactivation of dissolved oxygen in solvents and observed the formation of a defect-state E_{11}^- peak near 1134 nm (Figure S11). These results confirm that the formation of defect PL for SDS-SWCNT samples with 1 mass% SDS and 302 nm wavelength UV irradiation is due to the covalent SWCNT functionalization resulting from the aryl diazonium reaction, with minimal to no contribution from the oxygen doping of nanotubes.

Specifically, we observed a strong solvent-dependent aryl diazonium reaction with SWCNTs, where an order of magnitude higher concentrations of diazonium reactants were required to create OCC-tailored SWCNTs in H_2O

https://doi.org/10.1021/jacs.3c07341
J. Am. Chem. Soc. 2023, 145, 25621−25631

than in D_2O upon testing a broad concentration range of OCH_3-BDT (Figure 2, Figures S12 and S13, and Tables S2 and S3). We plotted the fluorescence spectra of covalently functionalized SWCNT samples as a function of increasing molar reactant ratios of [OCH_3-BDT]:[SWCNT carbon] in both solvents (Figure 2a,b and Figure S13a,b). The corresponding normalized PL obtained from the pristine E_{11} emission peak near 988 nm and defect PL near 1131 nm (i.e., corresponding to E_{11}^- band), which is red-shifted roughly by 143 nm (i.e., optical gap $\Delta E = E_{11} - E_{11}^-$ of 159 meV), is shown in Figure 2c,d. The normalization of pristine E_{11} and defect PL of reacted SWCNTs was performed by dividing by SF_0 (i.e., the initial E_{11} emission spectral flux of SWCNT samples without diazonium and UV irradiation) and SF_{max} (i.e., the maximum defect PL value) in H_2O and D_2O, respectively. Moderate redshifts of <200 meV are generally obtained for aryl diazonium reaction with near-armchair SWCNTs, such as (6,5) species. This is because the bonding of an aryl group at one carbon on the nanotube lattice leads to the predominant selectivity for the ortho^{++} bonding configuration of a pairing group, which attaches at an adjacent carbon closest to the SWCNT circumference.[9,20,44] As expected, we observed an exponential decrease of the pristine E_{11} emission, accompanied by the formation of defect PL, with the increasing concentration of diazonium reactants due to the trapping of mobile E_{11} excitons at the newly generated defect sites (Figure 2a−d and Figure S13).[5] However, the E_{11} emission decreases more drastically at a rate constant k (in units of (diazonium/carbon molar ratio)$^{-1}$) of 2.70 in D_2O, as compared to that of 0.34 in H_2O based on single exponential fits, over the entire concentration range of diazonium reactants tested in this work (Figure 2c). We also performed control experiments at [OCH_3-BDT]:[SWCNT carbon] = 3:1 using both DNA-SWCNTs without surfactant exchange and SDS-SWCNTs with membrane filtration, which removes the small amount of displaced, unbound DNA (Figure S14). For SDS-SWCNTs with and without membrane filtration, we observed similar degrees of relative doping (i.e., ∼86% in H_2O and ∼92% in D_2O), while the DNA-SWCNTs showed lower values (i.e., ∼46% in H_2O and ∼62% in D_2O). Moreover, the defect PL for SDS-SWCNTs is significantly larger (i.e., ∼8 times) than that for DNA-SWCNTs (centered around 1145 nm). These results suggest that the small amount of displaced, unbound DNA in solutions has a minimal effect on the aryl diazonium reaction with SDS-SWCNTs. Additionally, they provide evidence that the surfactant exchange of DNA-SWCNTs has resulted in displacing the DNA coating, which likely acts as a protective layer around SWCNTs minimizing the sidewall functionalization of nanotubes as reported previously for various reactions, including the aryl diazonium reaction.[37,45,46]

Surprisingly, the defect PL near 1131 nm shows outstanding stability and brightness in H_2O over a wide range of diazonium concentrations up to [OCH_3-BDT]/[SWCNT carbon] = 25 (i.e., 25:1) before significant fluorescence quenching occurs at [OCH_3-BDT]/[SWCNT carbon] = 45 (i.e., 45:1) (Figure 2d). This is indicated by the monotonic increase of the defect PL as a function of increasing molar reactant ratios at a rate constant $k \approx 0.56$ (in units of (diazonium/carbon molar ratio)$^{-1}$), before reaching a plateau near [OCH_3-BDT]/[SWCNT carbon] = 4 (i.e., 4:1) (Figure 2d). At [OCH_3-BDT]/[SWCNT carbon] = 8 (i.e., 8:1) and above, we observed a significant broadening of the defect PL peak in H_2O as indicated by the drastic increase in the full width at half-maximum (fwhm) values (Figure S13c). This corresponds to the formation of a clearly identifiable second, more red-shifted defect E_{11}^-* peak near 1210 nm (i.e., $\Delta E \approx 234$ meV) (Table S2). The appearance of a second E_{11}^-* peak possibly arises from a different bonding configuration of ortho$^+$, for which the functionalization bond is aligned away from the circumference.[9,12,21,44] Recent studies suggested para configuration (three carbons away) for a second E_{11}^-* emission, which formed simultaneously with E_{11}^- peak, for SWCNTs functionalized with aromatic reactants via triplet-state photochemistry in the absence of dissolved oxygen.[30,31] Additionally, the E_{11}^-* emission formed with bulky OCC defect pairs was assigned as para configuration due to the steric hindrance effect.[8] Although it is unlikely that the E_{11}^-* peak relates to the para configuration in our material system, which involves dissolved oxygen and OCC defect pairs with smaller steric size, the accurate assignment of the bonding configuration is worthy of future studies. Additionally, the defect E_{11}^- peak red-shifted by ∼7 nm, with concomitant blueshift of pristine E_{11} peak by ∼5 nm, accompanying the rise of E_{11}^-* peak in H_2O (Table S2). This type of two defect-state emission bands (i.e., E_{11}^- and E_{11}^-*) is common in ensemble PL spectra, particularly at high concentrations of diazonium due to a directing effect of existing defects for generating preferential bonding configuration for additional defect sites in close proximity.[12] Although minor due to the challenge in measuring the extremely dilute concentration of SWCNTs, we observed the appearance of a Raman disorder (D) peak near 1300 cm^{-1} with a corresponding D/G peak ratio (G band near 1590 cm^{-1}) of roughly 0.05 for the resulting OCC-tailored SWCNTs in H_2O at [OCH_3-BDT]/[SWCNT carbon] = 10 (i.e., 10:1), compared to the no obvious formation of a D peak at 0.01 (i.e., 1:100), suggesting the generation of higher defect density (Figure S15a and Table S4).

In comparison, the defect PL feature near 1131 nm and its brightening from aryl diazonium reactions in D_2O were obtained within a narrow window of molar reactant ratios, a trend consistent with previous reports (Figure 2d).[7,28] Specifically, the defect PL increased significantly as a function of increasing molar reactant ratios at a rate constant $k \approx 6.69$ (in units of (diazonium/carbon molar ratio)$^{-1}$) (i.e., ∼11.9 times larger than that in H_2O) up to [OCH_3-BDT]/[SWCNT carbon] = 1 (i.e., 1:1), followed by a drastic decrease above [OCH_3-BDT]/[SWCNT carbon] = 3 (i.e., 3:1) in D_2O (Figure 2d). This is possibly due to the excessive functionalization of SWCNTs compared to the reaction in H_2O, causing irreversible quenching of defect PL.[7,13] Additionally, we observed the onset of significant broadening of defect PL peak in D_2O at [OCH_3-BDT]/[SWCNT carbon] = 3 (i.e., 3:1) due to the formation of the second E_{11}^-* peak (Figure S13c and Table S3). The appearance of the D peak in Raman spectra and the increase in the D/G peak ratio from roughly 0.04 to 0.08 at an increasing molar reactant ratio from [OCH_3-BDT]/[SWCNT carbon] = 0.01 (i.e., 1:100) to 10 (i.e., 10:1) also indicate the formation of the resulting OCC-tailored SWCNTs in D_2O (Figure S15b). It is also important to note that the overall concentration of diazonium used to create OCC-tailored SWCNTs in D_2O by UV irradiation of diazonium, which is performed in this work, is several orders of magnitude higher than those obtained in previous reports where reactions were performed either in the dark or by exciting the SWCNTs using visible light.[7,28] Additionally, the

https://doi.org/10.1021/jacs.3c07341
J. Am. Chem. Soc. 2023, 145, 25621−25631

ratios of defect PL (near 1131 nm) over pristine E_{11} peak emission (i.e., corresponding to reacted SWCNTs with diazonium and UV irradiation) of OCC-tailored SWCNTs obtained in this work are roughly 18 in H_2O and 14 in D_2O, respectively, near the [OCH_3-BDT]:[SWCNT carbon] molar ratios (i.e., 10:1 in H_2O and 1:1 in D_2O, respectively) with maximum defect PL. As a comparison, the ratio of defect PL over E_{11} peak emission was ∼21 for OCC-tailored (6,5) SWCNTs formed from visible light excitation.[28]

The drastic difference in the amount of diazonium reactants needed for creating OCC-tailored SWCNTs suggests that solvent waters play an important role in aryl diazonium chemistry. As a direct comparison, we plotted the normalized fluorescence spectra of reacted (6,5) SWCNT samples at a molar ratio of [OCH_3-BDT]:[SWCNT carbon] = 1:10 in H_2O and D_2O, respectively (Figure 2e). The spectral normalization was performed by dividing the fluorescence spectra of reacted SWCNTs by the initial E_{11} emission spectral flux of SF_0 (i.e., corresponding to SWCNTs without diazonium and UV irradiation) in H_2O and D_2O, respectively. We observed the formation of a dominant defect-state E_{11}^- peak for the sample in D_2O, while no obvious, red-shifted peak was obtained for the sample in H_2O at this specific diazonium concentration. Additionally, we plotted the relative doping degree of OCC-SWCNTs produced in each solvent as a function of increasing molar reactant ratio (Figure 2f). In D_2O, the starting point of an exponential increase in the relative doping degree of SWCNTs occurred around [OCH_3-BDT]/[SWCNT carbon] = 0.005 (i.e., 1:200) compared to that of [OCH_3-BDT]/[SWCNT carbon] = 0.1 (i.e., 1:10) in H_2O. This corresponds to a diazonium molar concentration as high as roughly 20 times in H_2O than in D_2O, at the given SWCNT concentration (i.e., ∼0.85 μg/mL) tested in this work.

To further compare the rate of reaction of (6,5) SWCNTs in these solvents, we fitted the equilibrium (steady-state) aryl diazonium reaction with SWCNTs as a function of increasing molar reactant ratio using a well-established two-step adsorption−reaction model developed by Strano and colleagues (Figure 2f, eq 1).[1,4,47] Particularly, the cationic diazonium ions physically adsorb onto the surface of anionic surfactant-coated SWCNTs primarily through the electrostatic interactions, followed by the covalent attachment of aryl adducts onto the carbon lattice.[4] Specifically[4]

$$f_{(6,5)} = \frac{AK_AK_RC_0}{1/\theta_{TA} + K_AK_RC_0 + K_Al} \quad (1)$$

where $f_{(6,5)}$ is the relative doping degree of (6,5) SWCNTs (dimensionless), A is the maximum extent of doping (dimensionless), K_A is the adsorption constant (dimensionless), K_R is the reaction constant (in units proportional to nm per diazonium/water molar ratio), C_0 is the initial concentration of the diazonium salt added to the SWCNT samples (in units of diazonium/carbon molar ratio), θ_{TA} is the total number of available adsorption sites (i.e., $\theta_{TA} = \theta_{EA} + \theta_A$, where θ_{EA} is the number of empty adsorption sites available to the diazonium ions and θ_A is the number of sites occupied by the adsorbed diazonium ions) on the nanotube (in units of diazonium/water molar ratio per nm), and l is the total length of (6,5) SWCNTs in solution (in units of nm).

Table 1 shows the estimates of θ_{TA}, K_R, and A from data fitting, using a previously reported K_A value (i.e., ∼1640) for SDS-coated SWCNTs in an aqueous environment[4] and a calculated l value for the (6,5) SWCNT sample (i.e., ∼1.43 × 10^{14} nm) (see the Supporting Information). The difference in the linear packing density of diazonium ions on the SWCNT surface, θ_{TA}, is smaller (i.e., ∼1.98 times larger in D_2O than in H_2O) compared to the reaction constant K_R (i.e., ∼18.2 times larger in D_2O than in H_2O), while the saturated extent of doping, A, is the same for reactions performed in both solvents (Table 1). These results suggest that solvent isotope effects potentially impact the aryl diazonium reaction with SWCNTs, where the solvent waters participate in the reactions possibly through the breaking of O−H and O−D bonds, respectively.[48,49] It is also important to point out that D_2O (deuteration degree of ≥99.9%) was used in SWCNT reactions. There is residual H_2O, and some H_2O might be introduced due to water absorption during sample preparation. This tiny amount of H_2O has negligible impact on the overall SWCNT reactions. Based on the ^1H NMR spectrum measurements of solvents, D_2O showed a narrowed residual H_2O peak compared to the broader peaks of D_2O/H_2O mixed solvents (v/v) containing higher H_2O contents of 10% and 90%, respectively (Figure S16). Additionally, we performed SWCNT reactions in D_2O/H_2O mixed solvents (v/v) containing 1% and 10% of H_2O, resulting in slightly smaller degrees of relative doping (i.e., ∼95% and 91% in mixed solvents containing 1% and 10% H_2O, respectively) compared to that (i.e., ∼96%) in D_2O only (Figure S17). These results suggest that the D_2O solvent used in this work for SWCNT reactions contains less than 1% residue H_2O and its impact on the covalent SWCNT functionalization is negligible (Figures S16 and S17). Additionally, the solvent effects were observed for a different diazonium salt (i.e., COOH-BDT) reacting with SWCNTs, where OCC-tailored SWCNTs with bright defect PL near 1141 nm (i.e., $\Delta E \approx 171$ meV) were obtained at a higher concentration of diazonium in H_2O than in D_2O for different [COOH-BDT]:[SWCNT carbon] values of 1:10 and 6:1 tested (Figure S18).

Table 1. Summary of θ_{TA}, K_R, and A Values Deduced from Curve Fitting of the Relative Doping Degree of OCC-Tailored SWCNTs

Solvent	θ_{TA}	K_R	A
H_2O	3.26×10^{-19}	2.22×10^{21}	1.00
D_2O	6.46×10^{-19}	4.05×10^{22}	1.00

Additionally, we found that the formation of fluorescent quantum defects is possible in the solvent pH of roughly 5−5.5, as the defect-state E_{11}^- peak did not form for SWCNT samples in D_2O with a pH of 6.88 before pH adjustment (Figure S19). This is likely due to the slightly acidic conditions being able to promote the preservation of the cationic aryl diazonium moiety and the formation of aryl radicals, both of which are required for creating OCC-tailored SWCNTs.[23,47,50] In comparison, SDS-SWCNTs in H_2O had pH 5.30 ± 0.15 after sample preparation and were used directly for the reactions. Based on our observations, we propose the following mechanism for the solvent isotope effects on the aryl diazonium reaction with SWCNTs in aqueous environments (Figure 3). Initially, cationic diazonium ions physically adsorb onto the surface of SDS-SWCNTs, creating a stable non-covalently bound intermediate, a step that is known to occur in roughly 2.4 min.[1] The covalent attachment of aryl groups on the SWCNT surface is primarily induced by illuminating the samples with high-energy UV photon, thus generating highly

https://doi.org/10.1021/jacs.3c07341
J. Am. Chem. Soc. 2023, 145, 25621−25631

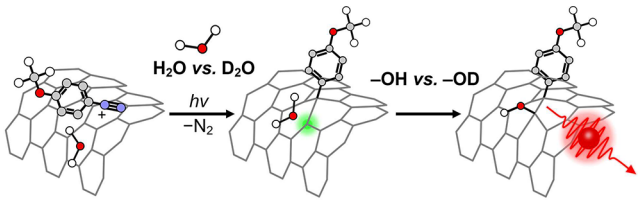

Figure 3. Reaction scheme for creating OCC-tailored SWCNTs by covalent functionalization of sp^2 carbon that incorporates aryl and pairing (e.g., −OH versus −OD) groups in water solvents with UV irradiation. The pairing group is shown in an ortho bonding configuration. The diazonium salt is OCH_3-BDT.

reactive aryl radicals that react with SWCNTs.[50,51] Furthermore, the creation of stable sp^3 fluorescent quantum defects on the sp^2 hybridized carbon lattice by implanting the aryl group is accompanied by introducing a pairing group from the solvent water, possibly −OH versus −OD (Figure 3). The possible generation of aryl radicals was also confirmed by the disappearance of the diazonium absorption peak at 314 nm with UV light irradiation (Figure S4).[32] In comparison, the absorption feature of diazonium remained unchanged when samples were left in the dark at ambient conditions (Figures S3 and S4).

Our material system clearly showed the two-step adsorption−reaction mechanism previously demonstrated for the aryl diazonium chemistry of SWCNTs.[1,4] Specifically, we found that the adsorption of diazonium on the surface of SDS-SWCNTs led to a stable and long-lived noncovalently bound intermediate as reported previously.[1] Upon addition of diazonium, we observed different levels of pristine PL quenching at the E_{11} peak without UV irradiation (Figure 4, Figure S20, and Table S5). The PL quenching is likely caused by the charge transfer between the semiconducting (6,5) SWCNTs and the adsorbed, electron-withdrawing aryl diazonium dopants (i.e., OCH_3-BDT).[1,2,30] At lower diazonium concentrations (e.g., [OCH_3-BDT]:[SWCNT carbon] = 1:25 and 1:10), we observed larger PL quenching of the E_{11} emission in H_2O than in D_2O (Figure 4 and Table S5). This could be due to slightly more diazonium ions being adsorbed on the nanotube surface (i.e., relating to larger θ_A) in H_2O as compared to that of D_2O, as solvent molecules may compete with diazonium ions in interacting with nanotubes. Additionally, the adsorption of diazonium ions may lead to the rearrangement of surfactant molecules locally on the nanotube surface due to electrostatic interactions between the cationic diazo group and the anionic SDS head groups.[4] The rearrangement behavior of surfactants may be different in H_2O versus D_2O. However, we observed minimal spectra shifts (i.e., <2 nm) in both solvent waters indicating that the surfactant rearrangement (i.e., relating to changes in the surface coverage of nanotubes) resulting from diazonium adsorption has a minor impact on the SWCNT quenching (Table S5). At a high diazonium concentration (e.g., [OCH_3-BDT]:[SWCNT carbon] = 3:1), a complete PL quenching was obtained in both waters possibly due to the saturation of sites occupied by the adsorbed diazonium ions (i.e., θ_A) on the nanotube surface (Figure 4). Generally, we exposed freshly prepared SWCNT samples containing diazonium reactants to 302 nm UV light for 50 min to ensure the completion of reaction. However, measurements of SWCNT fluorescence spectra as a function of UV exposure time ranging from 2 to 90 min showed that the growth of defect-state E_{11}^- emission peaks were stabilized at roughly 20 min in both waters (Figure S21a−d). Similarly, the corresponding relative doping degree of SWCNTs with increasing UV irradiation time reached a plateau near 20 min, indicating that 20 min of UV light irradiation is sufficient to complete the diazonium reaction with (6,5) SWCNTs (Figure S21e).

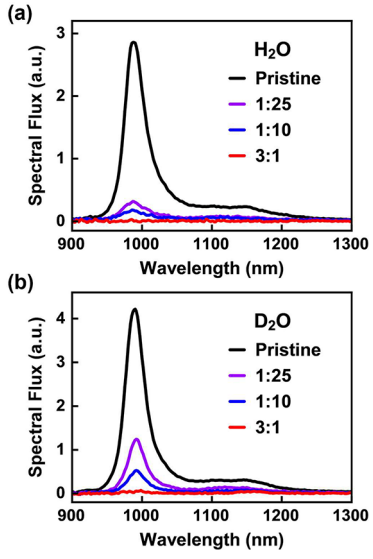

Figure 4. Fluorescence quenching of SWCNTs upon interaction with diazonium reactants without UV light irradiation. Fluorescence spectra of (6,5) SWCNT samples in (a) H_2O and (b) D_2O, respectively, before (i.e., pristine) and after mixing with diazonium at various molar reactant ratios of [OCH_3-BDT]:[SWCNT carbon].

Instead of irradiating the freshly prepared (6,5) SWCNT samples with UV light for 50 min, we first incubated the mixtures of SWCNTs and diazonium at [OCH_3-BDT]:[SWCNT carbon] = 3:1, where we observed the complete quenching of pristine E_{11} emission due to charge transfer with adsorbed diazonium, for 50 min in solvent waters, followed by exposing the mixtures to UV light at various time periods (Figure 5). We plotted the normalized fluorescence spectra of SWCNT samples by dividing the measured spectra by the initial E_{11} emission spectral flux of SF_0 (i.e., corresponding to SWCNTs without diazonium and UV irradiation) in H_2O and D_2O, respectively (Figure 5a,b). Within a short UV exposure time of 2 min, we observed the partial reversal of the pristine E_{11} (near 988 nm) emission, accompanied by the formation of a defect-state E_{11}^- peak (near 1131 nm) in both H_2O and D_2O, suggesting that UV light induces the conversion of the stable, noncovalently bound intermediate to covalently attached aryl adducts. The increase in normalized E_{11} PL values stabilized with 2 min of UV exposure, reaching roughly 47 ± 4% and 36 ± 2% of the SF_0 values of E_{11} emission in H_2O and D_2O, respectively (Figure 5c). The corresponding rate constant k (in units of min^{-1}) for increasing E_{11} emission is 1.61 in H_2O and 1.01 in D_2O, respectively, based on single exponential fits. In comparison, it took roughly 4 min of UV irradiation to stabilize the defect PL, reaching 64 ± 3% and 58 ± 1% of the SF_0 values of E_{11} emission in H_2O and D_2O, respectively (Figure 5c). The corresponding rate constant k (in units of min^{-1}) for increasing defect PL is 0.95 in H_2O and 0.68 in D_2O, respectively, based on single exponential fits. Additionally, the corresponding relative doping degrees of SWCNTs showed a sharp increase up to 2 min of UV irradiation before reaching

https://doi.org/10.1021/jacs.3c07341
J. Am. Chem. Soc. 2023, 145, 25621−25631

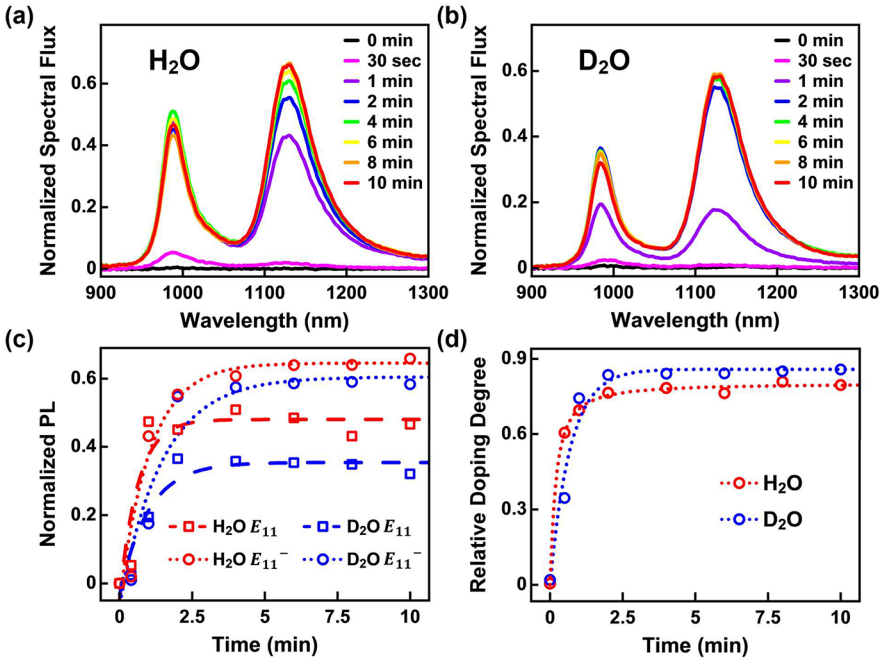

Figure 5. Time-dependent aryl diazonium chemistry of (6,5) SWCNTs with an OCH_3-BDT incubation. Normalized fluorescence spectra of (6,5) SWCNTs incubated with OCH_3-BDT for 50 min at a molar ratio of [OCH_3-BDT]:[SWCNT carbon] = 3:1 in (a) H_2O and (b) D_2O, followed by 302 nm UV light irradiation for various times. (c) Spectral evolution of the normalized intensities of pristine E_{11} (near 988 nm) and the defect-state E_{11}^- emission (near 1131 nm) as a function of UV irradiation time. The dotted lines in panel c represent the fitting curves with $R^2 \approx 94.4\%$ using single exponential fits (i.e., $y = Ae^{-kx} + B$, where A and B are correction factors). (d) Corresponding relative doping degree of (6,5) SWCNTs with time.

plateau values of 0.78 and 0.84 in H_2O and D_2O, respectively (Figure 5d). These results suggest that incubating the mixtures of SWCNTs and aryl reactants likely minimizes the effect of diazonium diffusion in the initial step of reaction with SWCNTs in solvents, thus allowing more efficient doping of SWCNTs at a shorter UV irradiation time.

Overall, we found significant water solvent isotope effects on the aryl diazonium reaction with SWCNTs in H_2O and D_2O, respectively. We propose two major factors that contribute to a larger reaction constant in D_2O than in H_2O: (i) the water interaction with SWCNTs and (ii) nucleophilic reactivity of water solvent on paring participation in the final step of the formation of the OCC-tailored SWCNTs. Ealier studies confirmed the deuterium attachment to SWCNTS in deuterated water and alcohols, indicating stronger deuterium−carbon interaction.[52,53] Another study found that deuterium shows stronger affinity toward SWCNTs, making D_2O a better solvent than H_2O.[54] Further, deuterated acid mixtures were found to enhance the solubility of SWCNTs,[55] which is attributed to the strong affinity for deuterium interactions with the nanotube surface. Therefore, we speculate that the stronger interaction of SWCNTs with D_2O contributes to a larger K_R value of aryl diazonium reaction with SWCNTs than in H_2O. This also correlates to our observation that stronger interaction of D_2O with SWCNTs has likely led to the lesser SWCNT quenching (i.e., relating to lesser adsorbed diazonium ions) during the first-step of reaction, that is, the physical adsorption of diazonium ions on the nanotube surface. Second, literature studies also confirmed that deuteroxide is both a stronger nucleophile and a base than hydroxide in several reactions, such as imidate hydrolysis[24] and detritiation of l,4-dicyano-2- butene-1-t.[56] Therefore, we anticipate that the K_R value for the reaction of the aryl-SWCNTs radical (or cation) with −OD is somewhat larger than that with −OH, despite less diazonium being adsorbed on the SWCNT surface. This also suggests that the second step of the reaction is the determining step in creating OCC-tailored SWCNTs, highlighting the important role of the solvent molecule in completing the covalent SWCNT functionalization by contributing a pairing group (possibly −OH versus −OD). Finally, the water solvent may affect the radical formation, reactivity, and stability under UV irradiation, which needs further studies. Efforts have been made to elucidate the chemical nature of pairing groups that are involved in the aryl diazonium reaction with SWCNTs both experimentally and theoretically.[6,8,19] However, direct experimental measurements of the pairing groups in our material systems remain a challenge and will be the topic of our future work.

CONCLUSIONS

The precision synthesis of OCC-tailored SWCNTs with defined structures and properties has been an emerging field in carbon nanotube chemistry for advancing applications such as optical sensing, imaging, and quantum information. We demonstrate the clearly distinguishable water solvent isotope effects on the aryl diazonium chemistry with SWCNTs using H_2O and D_2O, providing additional methods to control the creation of OCC-tailored SWCNTs. Particularly, UV-activated diazonium likely generates highly reactive aryl radicals, which can react with SWCNTs to form fluorescent quantum defects. This led to a roughly 18.2 times larger reaction constant in D_2O than in H_2O. Unlike a narrow window of reaction conditions in obtaining bright defect PL in D_2O, OCC-tailored SWCNTs in H_2O showed stable defect PL over a broad range of diazonium concentrations tested in this work. We propose

https://doi.org/10.1021/jacs.3c07341
J. Am. Chem. Soc. 2023, 145, 25621−25631

both the interaction of SWCNTs with water (H_2O vs D_2O) and nucleophilic reactivity of water solvent (H_2O vs D_2O) contribute to a larger reaction constant in the formation of OCC-tailored SWCNTs in D_2O than in H_2O. Additionally, we observed clearly identifiable steps of fluorescence quenching of SWCNTs followed by the defect PL formation with UV irradiation, showing strong evidence of the well-known two-step adsorption−reaction model of aryl diazonium reaction with SWCNTs. These findings reveal the important role of solvent water in the aryl diazonium chemistry of SWCNTs, providing additional controls for further functionalizing the OCC-tailored SWCNTs using chemistries, such as bioorthogonal chemistry, that require benign aqueous conditions.

EXPERIMENTAL SECTION

Purification of (6,5) SWCNTs. All experiments were performed utilizing pure-chirality (6,5) SWCNT species. The yield of purified (6,5) SWCNTs is roughly 2.1% based on the following procedure. Pure-chirality (6,5) SWCNT species was prepared using our previously reported polymer aqueous two-phase (ATP) separation method.[57,58] Specifically, CoMoCAT SWCNT powder (SG65i-L39, CHASM Advanced Materials) was dispersed using the resolving DNA sequence TTA TAT TAT ATT (Integrated DNA Technologies) in a total volume of 1 mL of deionized (DI) water (with a resistivity of 18 MΩ cm) containing 100 mM NaCl by probe tip sonication for 2 h at a power level of 8 W in an ice bath. Supernatant dispersions were collected after centrifugation at 17,000*g* for 90 min at 19 °C. The stock supernatant dispersions of DNA-SWCNTs were used for ATP separation of (6,5) SWCNT species.

The supernatant dispersion of DNA-SWCNTs was mixed with a stock polymer mixture solution containing 7.86% poly(ethylene glycol) (PEG) (MW ≈ 6 kDa, Alfa Aesar) and 10.71% dextran (DX) (MW ≈ 70 kDa, TCI Chemicals) at a volume ratio of DNA-SWCNT supernatant: stock PEG/DX mixture = 3:7. This yields final polymer concentrations of 5.50% PEG and 7.50% DX. Two-step separation of (6,5) SWCNTs was facilitated by adding poly(vinylpyrrolidone) (PVP, MW ≈ 10 kDa, Sigma-Aldrich), a DNA-SWCNT partition modulator, into the ATP mixture. For the first step of the separation, a final concentration of roughly 0.10% PVP was added to the ATP mixture to obtain highly enriched (6,5) species in the PEG-rich top phase. For the second step, we collected the (6,5)-enriched, PEG-rich top phase and added an equal volume of the blank DX-rich bottom phase (i.e., a polymer solution without SWCNTs) to form a new ATP system. A final concentration of 0.05% PVP was then added to isolate pure chirality (6,5) species in the PEG-rich top phase. All percentages specified for chemical concentrations are reported on a mass basis, unless indicated otherwise.

Polymers in purified (6,5) samples were removed using the SWCNT precipitation method reported previously.[37,59] Specifically, final concentrations of 0.5 M sodium thiocyanate (NaSCN, Sigma-Aldrich) and 100 μg/mL of excess DNA, which assist in maintaining the SWCNT dispersion stability, were added to the PEG-rich phase containing the purified (6,5) SWCNTs. The mixture was then incubated overnight at 4 °C before centrifugation at 17,000*g* for 30 min at 19 °C. After discarding the solvent, the (6,5) SWCNT pellet was washed five times using the corresponding solvent (i.e., DI H_2O and D_2O (deuteration degree ≥99.9%, Sigma-Aldrich), respectively) for photochemical reactions without disturbing the pellet. The (6,5) SWCNT pellet was then resuspended in H_2O and D_2O, respectively, by bath sonication for 30 min at room temperature. All samples containing D_2O were sealed during the sample preparation and reaction steps.

Displacing DNA Coating of (6,5) SWCNTs with Surfactant. Surfactant exchange of DNA-coated (6,5) SWCNTs was performed according to our previously reported method.[37] A final concentration of 1% sodium dodecyl sulfate (SDS, ≥99% BioXtra) solution was mixed with purified DNA-(6,5) SWCNT samples in H_2O and D_2O, respectively. The mixture was incubated in an oven at 40 °C for 10 min, followed by bath sonication for 10 min at room temperature to allow for the surfactant exchange to occur. Surfactant exchange was also performed using purified (6,5) SWCNTs wrapped by the TTA TAT TAT ATT sequence conjugated with 6-carboxyfluorescein (6-FAM) on the 3′ end of the DNA oligo (Integrated DNA Technologies). Subsequently, SDS-coated (6,5) SWCNTs were diluted using the corresponding solvent (i.e., H_2O and D_2O, respectively) with or without 1% SDS to yield final concentrations of 0.03% and 1% SDS, respectively. This yields SWCNT samples with an absorbance value of 0.13 ± 0.03 at the E_{11} peak wavelength of SDS-(6,5) SWCNTs near 990 nm using a 10 mm path length quartz cuvette, which corresponds to an approximately 0.85 μg/mL of SWCNT concentration[60] for photochemical reactions.

Synthesis of 4-Carboxylbenzene Diazonium Tetrafluoroborate Salt. The synthesis of 4-carboxylbenzene diazonium tetrafluoroborate (4-$C_6H_4COOHN_2^+ \cdot BF_4^-$ (i.e., COOH-BDT)) was performed using a reported method.[7] Briefly, 1.3 mL of tetrafluoroboric acid solution (HBF_4, Sigma-Aldrich, 48% in H_2O) was diluted by adding 1.5 mL of DI water in a glass vial, and the solution was allowed to cool in an ice bath with constant stirring for roughly 15 min. Then, 2.4 mM of 4-aminobenzoic acid powder ($NH_2C_6H_4COOH$, Sigma-Aldrich, ≥ 99%) was dissolved in the HBF_4 solution, followed by adding 4.8 M of aqueous solution of sodium nitrite ($NaNO_2$, Sigma-Aldrich, ≥97.9%) in a dropwise manner. The glass vial was kept in an ice bath during the entire reaction process. The reaction was completed upon formation of a white precipitate. The precipitated diazonium salt was washed using 150 mL of diethyl ether (Sigma-Aldrich, 1 ppm butylated hydroxytoluene (BHT) as inhibitor, anhydrous, ≥99.7%) under vacuum filtration for 15 min, while protecting the sample from the ambient light. (*Safety Note: All reaction steps were conducted under a fume hood ventilation. Potassium iodide starch paper was used to identify the generation of excess nitrous acid, which is known to cause violent decomposition.*)[61] The diazonium salt was stored at −20 °C in the absence of light and used within 5 days after synthesis. ^{1}H NMR spectrum measurements were performed at room temperature in D_2O solvent to characterize the 4-aminobenzoic acid and the synthesized diazonium salt COOH-BDT.

Oxygen Doping of SDS-(6,5) SWCNTs. Oxygen doping of SWCNTs with dissolved oxygen was performed using SDS-(6,5) SWCNT samples containing final concentrations of 0.03% and 1% SDS, respectively, in different solvents (i.e., H_2O and D_2O) according to our previously reported procedure.[37] Each reaction was performed using three replicates of samples. Briefly, (6,5) SWCNT samples were left exposed to ambient air in the dark for 30 min. The oxygen doping was performed using a quartz cuvette containing 0.2 mL of the (6,5) SWCNT sample. Cuvettes were sealed and exposed to ultraviolet (UV) light (3UV Lamp, cat# 95034, Thermo Scientific) of 254 and 302 nm wavelengths, respectively, at a power density of 3 mW/cm^2 for various time periods (i.e., 30, 50, 70, 90, and 120 min) at room temperature. The power density of UV light was measured using a UVP UVX Radiometer (Analytik Jena).

Aryl Diazonium Reaction of SDS-(6,5) SWCNTs. Aryl diazonium reaction of SWCNTs was performed using SDS-(6,5) SWCNT samples containing 1% SDS (including for samples incubated with diazonium reactants before exposure to UV light) in different solvents (i.e., H_2O and D_2O, respectively) under 302 nm wavelength UV light irradiation. The pH values of SDS-(6,5) SWCNT samples in D_2O were adjusted to pH 5.25 ± 0.25 using hydrochloric acid solution before reacting with aryl diazonium salts, while SDS-(6,5) samples in H_2O showed pH 5.30 ± 0.15 after surfactant exchange and were used directly for the reactions. We mainly utilized 4-methoxybenzenediazonium tetrafluoroborate (4-$C_6H_4OCH_3N_2^+ \cdot BF_4^-$ (i.e., OCH_3-BDT), Sigma-Aldrich, 98%) for testing various reaction conditions with SWCNTs. Samples containing diazonium salts were protected from ambient light during preparation. Specifically, stock solutions of OCH_3-BDT with varying concentrations of 0.5−50 mM in H_2O and D_2O, respectively, were prepared freshly before reacting with (6,5) SWCNTs. Small aliquots (i.e., <5 μL) of stock solutions of diazonium salt at various concentrations were added to the 0.5 mL of (6,5) SWCNT samples

https://doi.org/10.1021/jacs.3c07341
J. Am. Chem. Soc. 2023, 145, 25621−25631

in microcentrifuge test tubes, followed by pipet mixing. This yields mixtures of varying molar ratios of reactants [OCH_3-BDT]:[SWCNT carbon] from 1:400 to 60:1. The 0.3 mL of each mixture sample was transferred to a sealed quartz cuvette for the photochemical reaction using 302 nm wavelength UV light irradiation at a power density of 3 mW/cm^2 for 50 min at room temperature. The total sample preparation time preceding UV light irradiation was roughly 5 min, unless indicated otherwise. Membrane filtration of control SDS-SWCNT samples was performed using a Microcon centrifugal filter with a molecular weight cutoff (MWCO) of 100 kDa to remove a small amount of displaced, unbound DNA. The retentate after membrane filtration was washed with 1% SDS in H_2O and D_2O, respectively, eight times before redispersing in the corresponding 1% SDS solutions.

Additionally, the effect of UV light (302 nm wavelength) exposure time on the reaction outcome was tested using [OCH_3-BDT]:[SWCNT carbon] mixtures at molar ratios of 3:1 in H_2O and 1:10 in D_2O, respectively, at various time periods ranging from 2 to 90 min using three replicates. The solvent effect on the aryl diazonium reaction of SWCNTs was also demonstrated using the synthesized COOH-BDT salt. The stock solution of COOH-BDT was prepared at a concentration of 8.5 mM in H_2O and D_2O, respectively. The COOH-BDT salt was added to (6,5) SWCNTs at [COOH-BDT]:[SWCNT carbon] molar ratios of 1:10 and 3:1 in H_2O and D_2O, respectively, and exposed to 302 nm UV light for 50 min at room temperature.

Optical Spectroscopy Characterization. Optical spectroscopy characterization including vis−NIR absorbance (400−1600 nm), visible and NIR fluorescence (420−1600 nm), and Raman spectrum measurements of SWCNT samples were performed on an NS3 NanoSpectralyzer (Applied NanoFluorescence, LLC) using a 10 mm path length quartz cuvette. UV−vis absorbance measurements were performed using a Jasco V-760 spectrophotometer over a wavelength range of 187−800 nm. Fixed excitation wavelengths of 408 and 532 nm lasers, corresponding to the 6-FAM dye and E_{22} peak wavelength of (6,5) species, were used for acquiring visible and NIR fluorescence spectra of 6-FAM dye and SWCNTs, respectively. The measured pristine E_{11} and defect-state E_{11}^{-} and E_{11}^{-}* emission peaks of SWCNT samples were fitted with Voigt profiles (Figure S6).[62] The reported relative doping degree was obtained from the peak area ratio of spectrally integrated defect PL (>1045 nm) over the total fitted peaks of both the pristine and defect PL. Additionally, the area contribution from the E_{11} emission sideband[63] was removed from the fitted peak area of the defect PL.

■ ASSOCIATED CONTENT

Supporting Information

The Supporting Information is available free of charge at https://pubs.acs.org/doi/10.1021/jacs.3c07341.

Spectroscopic characterization of SWCNT samples, ^1H NMR and absorbance spectra of diazonium salts, calculation of the total length of SWCNTs in solution, and supplementary tables (PDF)

■ AUTHOR INFORMATION

Corresponding Authors

Xue-Long Sun − *Department of Chemical and Biomedical Engineering, Washkewicz College of Engineering, Cleveland State University, Cleveland, Ohio 44115, United States; Department of Chemistry, Center for Gene Regulation in Health and Disease (GRHD), Cleveland State University, Cleveland, Ohio 44115, United States;* orcid.org/0000-0001-6483-1709; Email: x.sun55@csuohio.edu

Geyou Ao − *Department of Chemical and Biomedical Engineering, Washkewicz College of Engineering, Cleveland State University, Cleveland, Ohio 44115, United States;* orcid.org/0000-0002-9932-3971; Email: g.ao@csuohio.edu

Authors

Brandon J. Heppe − *Department of Chemical and Biomedical Engineering, Washkewicz College of Engineering, Cleveland State University, Cleveland, Ohio 44115, United States*

Nina Dzombic − *Department of Chemical and Biomedical Engineering, Washkewicz College of Engineering, Cleveland State University, Cleveland, Ohio 44115, United States*

Joseph M. Keil − *Department of Chemistry, Center for Gene Regulation in Health and Disease (GRHD), Cleveland State University, Cleveland, Ohio 44115, United States*

Complete contact information is available at: https://pubs.acs.org/10.1021/jacs.3c07341

Notes

The authors declare no competing financial interest.

■ ACKNOWLEDGMENTS

We acknowledge the grants from the National Science Foundation (CBET-1917513 and REU Supplement and CAREER-2142579) and support of Cleveland State University (CSU) Faculty Research Development Fund (FRD). B.J.H acknowledges NASA Ohio Space Grant Consortium (OSGC) Undergraduate STEM Scholarship. We also acknowledge Ana M. DiLillo for help with (6,5) SWCNT purification.

■ REFERENCES

(1) Usrey, M. L.; Lippmann, E. S.; Strano, M. S. Evidence for a Two-Step Mechanism in Electronically Selective Single-Walled Carbon Nanotube Reactions. *J. Am. Chem. Soc.* **2005**, *127* (46), 16129−16135.

(2) Strano, M. S.; Dyke, C. A.; Usrey, M. L.; Barone, P. W.; Allen, M. J.; Shan, H.; Kittrell, C.; Hauge, R. H.; Tour, J. M.; Smalley, R. E. Electronic Structure Control of Single-Waited Carbon Nanotube Functionalization. *Science* **2003**, *301* (5639), 1519−1522.

(3) Blanch, A. J.; Lenehan, C. E.; Quinton, J. S. Dispersant Effects in the Selective Reaction of Aryl Diazonium Salts with Single-Walled Carbon Nanotubes in Aqueous Solution. *J. Phys. Chem. C* **2012**, *116* (2), 1709−1723.

(4) Lin, S.; Hilmer, A. J.; Mendenhall, J. D.; Strano, M. S.; Blankschtein, D. Molecular Perspective on Diazonium Adsorption for Controllable Functionalization of Single-Walled Carbon Nanotubes in Aqueous Surfactant Solutions. *J. Am. Chem. Soc.* **2012**, *134* (19), 8194−8204.

(5) Brozena, A. H.; Kim, M.; Powell, L. R.; Wang, Y. H. Controlling the Optical Properties of Carbon Nanotubes with Organic Colour-Centre Quantum Defects. *Nat. Rev. Chem.* **2019**, *3* (6), 375−392.

(6) Gifford, B. J.; Kilina, S.; Htoon, H.; Doorn, S. K.; Tretiak, S. Controlling Defect-State Photophysics in Covalently Functionalized Single-Walled Carbon Nanotubes. *Acc. Chem. Res.* **2020**, *53* (9), 1791−1801.

(7) Piao, Y.; Meany, B.; Powell, L. R.; Valley, N.; Kwon, H.; Schatz, G. C.; Wang, Y. Brightening of Carbon Nanotube Photoluminescence through the Incorporation of Sp^3 Defects. *Nat. Chem.* **2013**, *5* (10), 840−845.

(8) Wang, P.; Fortner, J.; Luo, H.; Kłos, J.; Wu, X.; Qu, H.; Chen, F.; Li, Y.; Wang, Y. H. Quantum Defects: What Pairs with the Aryl Group When Bonding to the Sp^2 Carbon Lattice of Single-Wall Carbon Nanotubes? *J. Am. Chem. Soc.* **2022**, *144* (29), 13234−13241.

(9) Saha, A.; Gifford, B. J.; He, X.; Ao, G.; Zheng, M.; Kataura, H.; Htoon, H.; Kilina, S.; Tretiak, S.; Doorn, S. K. Narrow-Band Single-Photon Emission through Selective Aryl Functionalization of Zigzag Carbon Nanotubes. *Nat. Chem.* **2018**, *10* (11), 1089−1095.

(10) Zaumseil, J. Luminescent Defects in Single-Walled Carbon Nanotubes for Applications. *Adv. Opt. Mater.* **2022**, *10* (2), 2101576.
(11) Gifford, B. J.; Kilina, S.; Htoon, H.; Doorn, S. K.; Tretiak, S. Exciton Localization and Optical Emission in Aryl-Functionalized Carbon Nanotubes. *J. Phys. Chem. C* **2018**, *122* (3), 1828−1838.
(12) Gifford, B. J.; He, X.; Kim, M.; Kwon, H.; Saha, A.; Sifain, A. E.; Wang, Y.; Htoon, H.; Kilina, S.; Doorn, S. K.; Tretiak, S. Optical Effects of Divalent Functionalization of Carbon Nanotubes. *Chem. Mater.* **2019**, *31* (17), 6950−6961.
(13) Sykes, M. E.; Kim, M.; Wu, X.; Wiederrecht, G. P.; Peng, L.; Wang, Y. H.; Gosztola, D. J.; Ma, X. Ultrafast Exciton Trapping at Sp^3 Quantum Defects in Carbon Nanotubes. *ACS Nano* **2019**, *13* (11), 13264−13270.
(14) Kim, M.; Adamska, L.; Hartmann, N. F.; Kwon, H.; Liu, J.; Velizhanin, K. A.; Piao, Y.; Powell, L. R.; Meany, B.; Doorn, S. K.; Tretiak, S.; Wang, Y. H. Fluorescent Carbon Nanotube Defects Manifest Substantial Vibrational Reorganization. *J. Phys. Chem. C* **2016**, *120* (20), 11268−11276.
(15) Kim, M.; Chen, C.; Wang, P.; Mulvey, J. J.; Yang, Y.; Wun, C.; Antman-Passig, M.; Luo, H.-B.; Cho, S.; Long-Roche, K.; Ramanathan, L. V.; Jagota, A.; Zheng, M.; Wang, Y. H.; Heller, D. A. Detection of Ovarian Cancer via the Spectral Fingerprinting of Quantum-Defect-Modified Carbon Nanotubes in Serum by Machine Learning. *Nat, Biomed. Eng.* **2022**, *6* (3), 267−275.
(16) Mandal, A. K.; Wu, X.; Ferreira, J. S.; Kim, M.; Powell, L. R.; Kwon, H.; Groc, L.; Wang, Y. H.; Cognet, L. Fluorescent Sp^3 Defect-Tailored Carbon Nanotubes Enable NIR-II Single Particle Imaging in Live Brain Slices at Ultra-Low Excitation Doses. *Sci. Rep.* **2020**, *10* (1), 5286.
(17) Luo, Y.; He, X.; Kim, Y.; Blackburn, J. L.; Doorn, S. K.; Htoon, H.; Strauf, S. Carbon Nanotube Color Centers in Plasmonic Nanocavities: A Path to Photon Indistinguishability at Telecom Bands. *Nano Lett.* **2019**, *19* (12), 9037−9044.
(18) He, X.; Hartmann, N. F.; Ma, X.; Kim, Y.; Ihly, R.; Blackburn, J. L.; Gao, W.; Kono, J.; Yomogida, Y.; Hirano, A.; Tanaka, T.; Kataura, H.; Htoon, H.; Doorn, S. K. Tunable Room-Temperature Single-Photon Emission at Telecom Wavelengths from Sp^3 Defects in Carbon Nanotubes. *Nat. Photonics* **2017**, *11* (9), 577−582.
(19) He, X.; Gifford, B. J.; Hartmann, N. F.; Ihly, R.; Ma, X.; Kilina, S. V.; Luo, Y.; Shayan, K.; Strauf, S.; Blackburn, J. L.; Tretiak, S.; Doorn, S. K.; Htoon, H. Low-Temperature Single Carbon Nanotube Spectroscopy of Sp^3 Quantum Defects. *ACS Nano* **2017**, *11* (11), 10785−10796.
(20) Kim, M.; Wu, X.; Ao, G.; He, X.; Kwon, H.; Hartmann, N. F.; Zheng, M.; Doorn, S. K.; Wang, Y. H. Mapping Structure-Property Relationships of Organic Color Centers. *Chem.* **2018**, *4* (9), 2180−2191.
(21) Qu, H.; Wu, X.; Fortner, J.; Kim, M.; Wang, P.; Wang, Y. H. Reconfiguring Organic Color Centers on the Sp^2 Carbon Lattice of Single-Walled Carbon Nanotubes. *ACS Nano* **2022**, *16* (2), 2077−2087.
(22) Luo, H.-B.; Wang, P.; Wu, X.; Qu, H.; Ren, X.; Wang, Y. One-Pot, Large-Scale Synthesis of Organic Color Center-Tailored Semiconducting Carbon Nanotubes. *ACS Nano* **2019**, *13* (7), 8417−8424.
(23) Schmidt, G.; Gallon, S.; Esnouf, S.; Bourgoin, J. P.; Chenevier, P. Mechanism of the Coupling of Diazonium to Single-Walled Carbon Nanotubes and Its Consequences. *Chemistry* **2009**, *15* (9), 2101−2110.
(24) Pocker, Y.; Beug, M. W.; Stephens, K. L. Phenyl N-Methylacetimidate in H_2O and D_2O and Its Reactions with Nucleophiles. *J. Am. Chem. Soc.* **1974**, *96* (1), 174−180.
(25) Plonka, A.; Kevan, L. Solvent Isotope Effect on the Reactivity of Photoproduced Cations Embedded in Micelles. *J. Phys. Chem.* **1984**, *88* (25), 6348−6350.
(26) Battigelli, A.; Almeida, B.; Shukla, A. Recent Advances in Bioorthogonal Click Chemistry for Biomedical Applications. *Bioconjugate Chem.* **2022**, *33* (2), 263−271.
(27) Bertozzi, C. R. A Decade of Bioorthogonal Chemistry. *Acc. Chem. Res.* **2011**, *44* (9), 651−653.
(28) Powell, L. R.; Piao, Y.; Wang, Y. Optical Excitation of Carbon Nanotubes Drives Localized Diazonium Reactions. *J. Phys. Chem. Lett.* **2016**, *7* (18), 3690−3694.
(29) Wu, X.; Kim, M.; Kwon, H.; Wang, Y. Photochemical Creation of Fluorescent Quantum Defects in Semiconducting Carbon Nanotube Hosts. *Angew. Chem.* **2018**, *130* (3), 656−661.
(30) Zheng, Y.; Bachilo, S. M.; Weisman, R. B. Photoexcited Aromatic Reactants Give Multicolor Carbon Nanotube Fluorescence from Quantum Defects. *ACS Nano* **2020**, *14* (1), 715−723.
(31) Zheng, Y.; Han, Y.; Weight, B. M.; Lin, Z.; Gifford, B. J.; Zheng, M.; Kilin, D.; Kilina, S.; Doorn, S. K.; Htoon, H.; Tretiak, S. Photochemical Spin-State Control of Binding Configuration for Tailoring Organic Color Center Emission in Carbon Nanotubes. *Nat. Commun.* **2022**, *13* (1), 4439.
(32) Evleth, E. M.; Cox, R. J. Assignments of the Electronic Transitions in the Methoxy-Substituted Benzenediazonium Cations. *J. Phys. Chem.* **1967**, *71* (12), 4082−4089.
(33) Ambroz, H. B.; Przybytniak, G. K.; Stradowski, C.; Wolszczak, M. Optical Spectroscopy of the Aryl Cation, the Intermediate in the Decomposition of Arenediazonium Salts. *J. Photochem. Photobiol., A* **1990**, *52* (3), 369−374.
(34) Ambroz, H. B.; Kemp, T. J.; Przybytniak, G. K. Optical Spectroscopy of the Aryl Cation Part 2. Matrix Effects on the Production of 3Ar+. *J. Photochem. Photobiol., A* **1991**, *60* (1), 91−99.
(35) Gasper, S. M.; Schuster, G. B.; Devadoss, C. Photolysis of Substituted Benzenediazonium Salts: Spin-Selective Reactivity of Aryl Cations. *J. Am. Chem. Soc.* **1995**, *117* (19), 5206−5211.
(36) Witzel, S.; Hoffmann, M.; Rudolph, M.; Kerscher, M.; Comba, P.; Dreuw, A.; Hashmi, A. S. K. Excitation of Aryl Cations as the Key to Catalyst-Free Radical Arylations. *Cell Rep. Phys. Sci.* **2021**, *2* (2), 100325.
(37) Xhyliu, F.; Ao, G. Surface Coating- and Light-Controlled Oxygen Doping of Carbon Nanotubes. *J. Phys. Chem. C* **2021**, *125* (17), 9236−9243.
(38) Tummala, N. R.; Striolo, A. SDS Surfactants on Carbon Nanotubes: Aggregate Morphology. *ACS Nano* **2009**, *3* (3), 595−602.
(39) Zhang, J.; Landry, M. P.; Barone, P. W.; Kim, J. H.; Lin, S.; Ulissi, Z. W.; Lin, D.; Mu, B.; Boghossian, A. A.; Hilmer, A. J.; et al. Molecular Recognition Using Corona Phase Complexes Made of Synthetic Polymers Adsorbed on Carbon Nanotubes. *Nat. Nanotechnol.* **2013**, *8* (12), 959−968.
(40) Yang, R.; Jin, J.; Chen, Y.; Shao, N.; Kang, H.; Xiao, Z.; Tang, Z.; Wu, Y.; Zhu, Z.; Tan, W. Carbon Nanotube-Quenched Fluorescent Oligonucleotides: Probes That Fluoresce upon Hybridization. *J. Am. Chem. Soc.* **2008**, *130* (26), 8351−8358.
(41) Gravely, M.; Safaee, M. M.; Roxbury, D. Biomolecular Functionalization of a Nanomaterial to Control Stability and Retention within Live Cells. *Nano Lett.* **2019**, *19* (9), 6203−6212.
(42) Lin, C.-W.; Bachilo, S. M.; Zheng, Y.; Tsedev, U.; Huang, S.; Weisman, R. B.; Belcher, A. M. Creating Fluorescent Quantum Defects in Carbon Nanotubes Using Hypochlorite and Light. *Nat. Commun.* **2019**, *10* (1), 2874.
(43) Farooq, Z.; Chestakov, D. A.; Yan, B.; Groenenboom, G. C.; van der Zande, W. J.; Parker, D. H. Photodissociation of Singlet Oxygen in the UV Region. *Phys. Chem. Chem. Phys.* **2014**, *16* (7), 3305.
(44) Gifford, B. J.; Saha, A.; Weight, B. M.; He, X.; Ao, G.; Zheng, M.; Htoon, H.; Kilina, S.; Doorn, S. K.; Tretiak, S. Mod(n-m,3) Dependence of Defect-State Emission Bands in Aryl-Functionalized Carbon Nanotubes. *Nano Lett.* **2019**, *19* (12), 8503−8509.
(45) Palma, M.; Wang, W.; Penzo, E.; Brathwaite, J.; Zheng, M.; Hone, J.; Nuckolls, C.; Wind, S. J. Controlled Formation of Carbon Nanotube Junctions via Linker-Induced Assembly in Aqueous Solution. *J. Am. Chem. Soc.* **2013**, *135* (23), 8440−8443.
(46) Clément, P.; Trinchera, P.; Cervantes-Salguero, K.; Ye, Q.; Jones, C.; Palma, M. A One-Step Chemical Strategy for the Formation

https://doi.org/10.1021/jacs.3c07341
J. Am. Chem. Soc. 2023, 145, 25621−25631

of Carbon Nanotube Junctions in Aqueous Solution: Reaction of DNA-Wrapped Carbon Nanotubes with Diazonium Salts. *ChemPlusChem.* **2019**, *84* (9), 1235−1238.
(47) Hilmer, A. J.; McNicholas, T. P.; Lin, S.; Zhang, J.; Wang, Q. H.; Mendenhall, J. D.; Song, C.; Heller, D. A.; Barone, P. W.; Blankschtein, D.; Strano, M. S. Role of Adsorbed Surfactant in the Reaction of Aryl Diazonium Salts with Single-Walled Carbon Nanotubes. *Langmuir* **2012**, *28* (2), 1309−1321.
(48) Sayler, A. M.; Leonard, M.; Carnes, K. D.; Cabrera-Trujillo, R.; Esry, B. D.; Ben-Itzhak, I. Preference for Breaking the O-H Bond over the O-D Bond Following HDO Ionization by Fast Ions. *J. Phys. B: At., Mol. Opt. Phys.* **2006**, *39* (7), 1701.
(49) Kumar, S.; Hoshino, M.; Kerkeni, B.; García, G.; LimãO-Vieira, P. Isotope Effect in D2O Negative Ion Formation in Electron Transfer Experiments: DO-D Bond Dissociation Energy. *J. Phys. Chem. Lett.* **2023**, *14* (23), 5362−5369.
(50) Kvasovs, N.; Gevorgyan, V. Contemporary Methods for Generation of Aryl Radicals. *Chem. Soc. Rev.* **2021**, *50* (4), 2244−2259.
(51) Witzel, S.; Hoffmann, M.; Rudolph, M.; Kerscher, M.; Comba, P.; Dreuw, A.; Hashmi, A. S. K. Excitation of Aryl Cations as the Key to Catalyst-Free Radical Arylations. *Cell Rep. Phys. Sci.* **2021**, *2* (2), 100325.
(52) Fu, K.; Li, H.; Zhou, B.; Kitaygorodskiy, A.; Allard, L. F.; Sun, Y. P. Deuterium Attachment to Carbon Nanotubes in Deuterated Water. *J. Am. Chem. Soc.* **2004**, *126* (14), 4669−4675.
(53) Fu, K.; Kitaygorodskiy, A.; Rao, A. M.; Sun, Y. P. Deuterium Attachment to Carbon Nanotubes in Solution. *Nano Lett.* **2002**, *2* (10), 1165−1168.
(54) Yang, Q.-H.; Gale, N.; Oton, C. J.; Li, H.; Nandhakumar, I. S.; Tang, Z.-Y.; Brown, T.; Loh, W. H. Deuterated Water as Super Solvent for Short Carbon Nanotubes Wrapped by DNA. *Carbon* **2007**, *45* (13), 2701−2703.
(55) Ramanathan, T.; Fisher, F. T.; Ruoff, R. S.; Catherine Brinson, L. Apparent Enhanced Solubility of Single-Wall Carbon Nanotubes in a Deuterated Acid Mixture. *Res. Lett. Nanotechnol.* **2008**, *2008*, 296928.
(56) Walters, E. A.; Long, F. A. Isotope Effects on Hydroxide Ion in Aqueous Solution. *J. Phys. Chem.* **1972**, *76* (3), 362−365.
(57) Ao, G.; Streit, J. K.; Fagan, J. A.; Zheng, M. Differentiating Left- and Right-Handed Carbon Nanotubes by DNA. *J. Am. Chem. Soc.* **2016**, *138* (51), 16677−16685.
(58) Ao, G.; Zheng, M. Preparation and Separation of DNA-Wrapped Carbon Nanotubes. *Curr. Protoc. Chem. Biol.* **2015**, *7* (1), 43−51.
(59) Khripin, C. Y.; Arnold-Medabalimi, N.; Zheng, M. Molecular-Crowding-Induced Clustering of DNA-Wrapped Carbon Nanotubes for Facile Length Fractionation. *ACS Nano* **2011**, *5* (10), 8258−8266.
(60) Zheng, M.; Diner, B. A. Solution Redox Chemistry of Carbon Nanotubes. *J. Am. Chem. Soc.* **2004**, *126* (47), 15490−15494.
(61) Sheng, M.; Frurip, D.; Gorman, D. Reactive Chemical Hazards of Diazonium Salts. *J. Loss Prev. Process Ind.* **2015**, *38*, 114−118.
(62) Pfohl, M.; Tune, D. D.; Graf, A.; Zaumseil, J.; Krupke, R.; Flavel, B. S. Fitting Single-Walled Carbon Nanotube Optical Spectra. *ACS Omega* **2017**, *2* (3), 1163−1171.
(63) Kadria-Vili, Y.; Bachilo, S. M.; Blackburn, J. L.; Weisman, R. B. Photoluminescence Side Band Spectroscopy of Individual Single-Walled Carbon Nanotubes. *J. Phys. Chem. C* **2016**, *120* (41), 23898−23904.

https://doi.org/10.1021/jacs.3c07341
J. Am. Chem. Soc. 2023, 145, 25621−25631